Rate Considerations in Deep Space Telemetry

M. Costa, M. Belongie, and F. Pollara
Communications Systems Research Section

The relationship between transmission rate and source and channel signal-to-noise ratios (SNRs) is discussed for the transmission of a Gaussian source over a binary input, additive Gaussian channel, with a mean-squared distortion criterion. We point out that for any finite rate, and sufficiently high channel SNR, the fidelity criterion (reproduction SNR) is upper bounded by a function of the transmission rate. Thus, the performance becomes rate limited rather than power limited. This effect is not observed with the binary symmetric source, the binary-input Gaussian channel combination, or the Gaussian source, unconstrained-input Gaussian channel combination.

I. Introduction

The deep space communication channel uses binary phase shift keying (BPSK) modulation and is well modeled as a binary input, additive white Gaussian noise (AWGN) channel model. It is usually accepted that there is no bandwidth constraint in deep space communication application and that, for sufficiently wide bandwidth usage, the full benefit of unconstrained bandwidth is essentially realized. While these notions are correct, they must be viewed with caution. It does not necessarily follow that, for sufficiently low overall transmission rate, there is little to be gained by further decreasing the rate. The interplay between source and channel coding and the issue of coding complexity need to be considered. Depending on the telemetry source and the available channel signal-to-noise ratio (SNR), there may be a significant advantage in further decreasing the rate.

In this article, we review these notions in the context of a deep space communication system with an independent identically distributed (i.i.d.) Gaussian source and a conventional BPSK, power-limited channel, using mean-squared error (MSE) as a distortion criterion. While not an accurate model for most deep space telemetry sources, the white Gaussian source is a useful reference model. Typical telemetry data can be transformed by an (approximately) decorrelating orthogonal transformation, such as the discrete cosine transform, producing data that can be approximated by parallel sources with white (generalized) Gaussian distributions of different variances, one for each transform coefficient. Thus, the combined source and channel coding of a white Gaussian source for transmission over the deep space channel is a relevant exercise.

II. Preliminaries

The well-known equations governing transmission rate and source and channel SNRs were established by Shannon in his seminal 1948 articles [1]. We refer to [2] as a source of notation. Figure 1 shows the system under consideration.

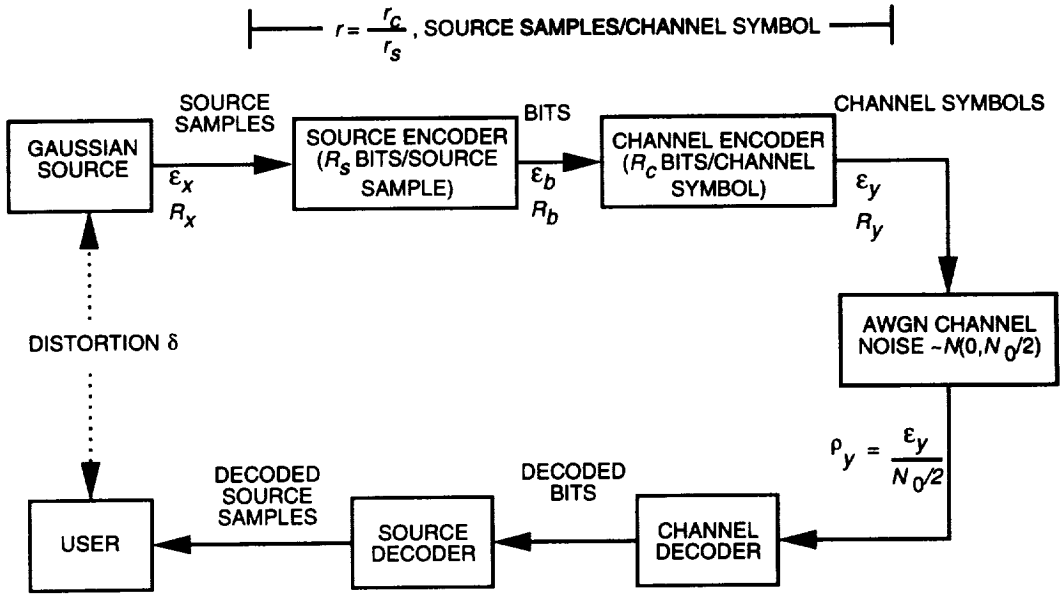

Fig. 1. Communication system model.

The capacity of a binary-input AWGN channel is given by

$$C(\rho_y) = 1 - E_u \left[\log_2(1 + e^{-2u})\right] \tag{1}$$

where $\rho_y = 2\mathcal{E}_y/N_0$, $\mathcal{E}_y$ is the available energy per channel symbol, $N_0/2$ is the two-sided noise spectral density, and E_u denotes expectation over u, a random variable with distribution $N(\rho_y, \rho_y)$.

The rate distortion function for an i.i.d. Gaussian source is given by

$$R(\delta) = \frac{1}{2}\log_2\left(\frac{1}{\delta}\right) \tag{2}$$

where δ is the normalized MSE distortion. The reproduction SNR (RSNR) is given by $1/\delta$.

III. Discussion

There are three variables of interest in this communication problem. They are

(1) δ, the normalized MSE distortion of reproduction at the receiver

(2) ρ_x, the available channel SNR, given by $\rho_x = 2\mathcal{E}_x/N_0$

(3) r, the overall transmission rate, measured in source samples per channel use

These quantities must satisfy the inequality

$$C(r\rho_x) \geq rR(\delta) \tag{3}$$

If the coding procedure is divided into a cascade of source and channel encoders, where the source is first converted into a string of binary symbols, the rate r satisfies

$$r = \frac{r_c}{r_s} = \frac{R_x}{R_y} \tag{4}$$

where r_s is the source code rate measured in bits per source sample, r_c is the channel code rate in information bits per channel use, R_x is the source rate in samples per second, and R_y is the channel rate in channel uses per second. Considering that each bandwidth unit (Hertz) corresponds, by the Nyquist sampling theorem, to two dimensions (channel uses) per second, we relate the bandwidth B to R_y by $B = R_y/2$.

Other channel SNRs of interest are ρ_b and ρ_y, the signal-to-noise ratios available per information bit and per channel use, respectively. We have selected ρ_x for our considerations because it is desirable to compare transmission schemes that use the same power and time to transmit each source sample. These three SNRs are related by $r\rho_x = r_c\rho_b = \rho_y$.

Substituting Eqs. (1) and (2) in Eq. (3), we can obtain the fundamental bound on RSNR given r and ρ_x:

$$\frac{r}{2}\log_2\left(\frac{1}{\delta}\right) \leq 1 - E_u\left[\log_2(1 + e^{-2u})\right] \tag{5}$$

where the distribution of u is now expressed as $N(r\rho_x, r\rho_x)$. This bound is depicted in Fig. 2, where we present plots of RSNR versus $\mathcal{E}_x/N_0$ for different values of overall rate r. (We use $\mathcal{E}_x/N_0$ instead of ρ_x in all the figures for consistency with [2] and other articles.)

In the limit as $r \to 0$, Eq. (5) becomes

$$\frac{1}{\delta} \leq e^{\rho_x} \tag{6}$$

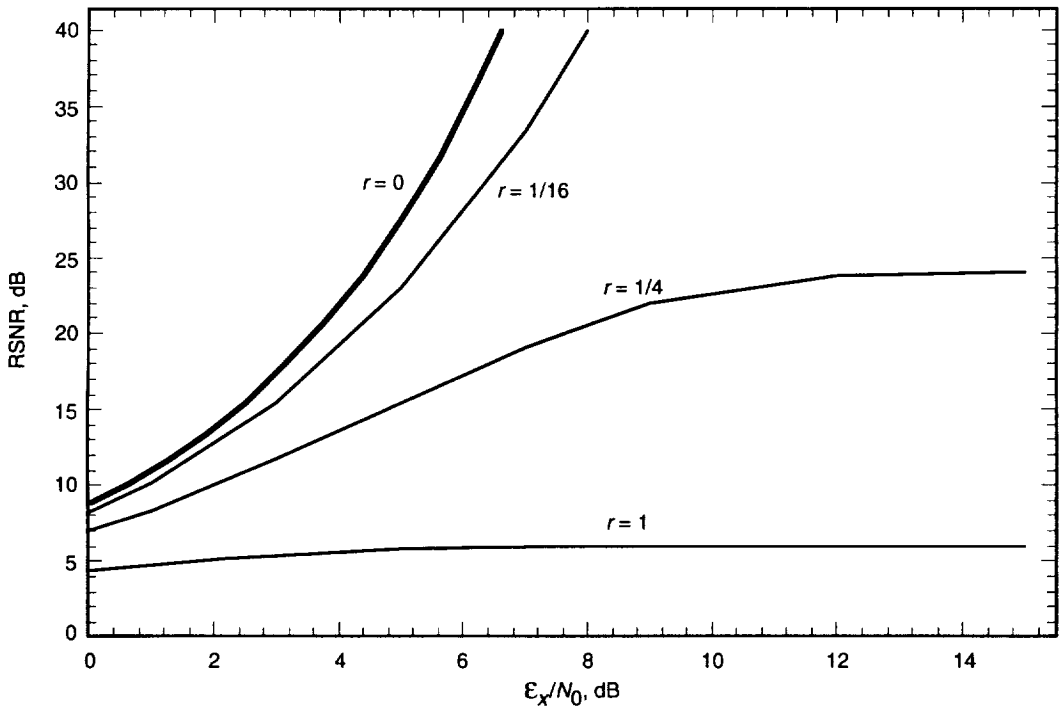

Fig. 2. Bounds on performance for a binary input channel with fixed *r*.

Thus, as ρ_x increases without bound, RSNR also may increase without bound. To increase ρ_x, one needs to alter the source transmission rate or the available power P. We have $\rho_x = P/R_x$. Thus, ρ_x can be increased by reducing the source rate R_x. This in turn affects the overall rate, since $r = R_x/R_y = R_x/2B$. Alternatively, ρ_x can be increased with an increase in P.

The noted unbounded growth in RSNR only occurs in the limit as $r \to 0$. For any positive value of r, the upper bound on RSNR approaches a finite limit as ρ_x increases. This occurs when ρ_x is large enough to make the channel essentially noiseless. Since the channel is restricted to binary input, its capacity is upper bounded by 1-bit-per-channel use. Thus, the RSNR is upper bounded by a function of the overall rate: $1/\delta < 2^{(2/r)}$. Since this bound can be arbitrarily smaller than the bound that prevails in the limit as $r \to 0$, Eq. (6), it is clear that the performance can greatly benefit from a decrease in overall rate (or an increase in bandwidth when R_x is held constant).

As shown in [3], the binary input AWGN channel has essentially the same performance as the unconstrained power-limited AWGN channel for low enough overall rates (e.g., less than 0.3 bit/channel use) when used to communicate a binary symmetric source. Interestingly, the same observation cannot be made for the case of communicating a Gaussian random variable, except in the limit as $r \to 0$. For any positive value of r, which suggests a finite level of complexity, and sufficiently high ρ_x, the binary input channel will have its performance (RSNR) limited by rate rather than by power. This effect is not observed in the unconstrained input AWGN case, where, for a fixed arbitrary rate, the upper bound on RSNR grows to ∞ as $\rho_x \to \infty$. Figure 3 compares, for various values of r, the unconstrained input and binary input cases. (The dotted lines are asymptotes.)

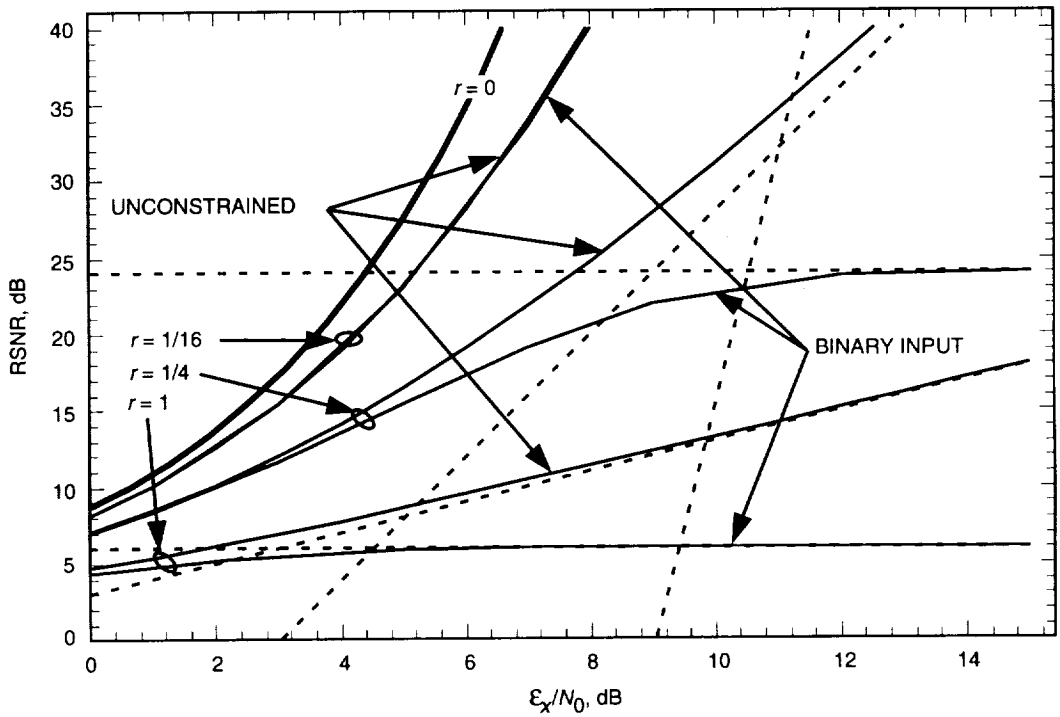

Fig. 3. Comparison of binary input channel and unconstrained channel for fixed *r*.

IV. Applicability

Under what circumstances might there be a lower bound on the overall rate r? This is a complicated issue, but we can make a few observations. First, any real system must have some nonzero value of r. Second, r clearly has some relationship to complexity, because $r = r_c/r_s$, and both lower-rate channel

codes and higher-rate source codes generally imply higher complexity. Thus, a constraint on r can be seen as a constraint on overall complexity. However, we can also consider the two components, r_s and r_c, separately. Fixing r_s explicitly puts an upper bound on RSNR, resulting in the bounds shown in Fig. 4. For this case, there is no difference between the unconstrained and binary input channels. Fixing r_c results in curves as shown in Fig. 5. Although a difference is seen between the unconstrained and binary input channels, the curves all have the same exponential shape. So, the interesting phenomenon described for fixed values of r (i.e., the different limiting behavior for binary input and unconstrained channels) depends on a simultaneous bound on r_s and r_c by fixing their ratio.

To see what implications this phenomenon might have, we must consider for which combinations of r, RSNR, and ρ_x it occurs. For a fixed value of r, the intercept of the asymptotes, as illustrated in Fig. 3, is approximately where the effect becomes significant. This intercept occurs at $\delta = 2^{-2/r}$ and $\rho_x = 4/r$. So, for instance, if $r = 1/4$, the effect becomes significant for RSNR > 24 dB and $\rho_x > 9$ dB. While these SNRs are certainly within the range of interest, it is hard to imagine reasonable circumstances requiring $r \geq 1/4$. For $r = 1/16$, which is known to be quite feasible for deep space communication, the effect becomes significant for RSNR > 96 dB and $\rho_x > 15$ dB. These SNRs are probably outside the range of interest of most missions.

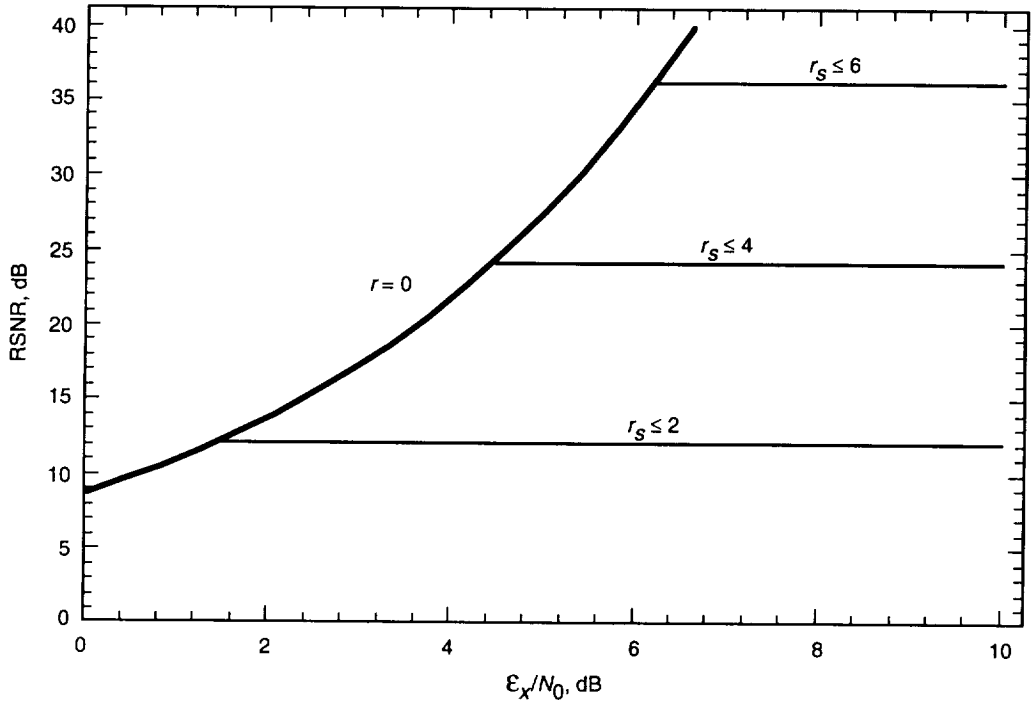

Fig. 4. Bounds on performance for binary input channel or unconstrained channel with r_s limited.

V. Performance Bounds With Fixed Channel SNR

Complexity is not the only reason that $r = 0$ is impossible. For a fixed ρ_x, $r \to 0$ implies $\rho_y \to 0$. Thus, even if the computational complexity of a very low-rate channel code or very high-rate source code is not a concern, the low SNR of the channel symbols might be. Although in theory ρ_y can be arbitrarily small as long as $C(\rho_y) > rR(\delta)$, in practice there is a lower bound on ρ_y below which any given receiver cannot perform symbol synchronization. Performance curves at constant ρ_y are shown in Fig. 6 for both the unconstrained and binary input channels. Since the curves are all exponential, we see that the differing

behavior between the unconstrained and binary input channels for fixed values of r is not due to a bound on ρ_y. It can also be seen from Fig. 6 that the performance difference between the unconstrained and binary input channels is negligible for $\rho_y < 0$ dB.

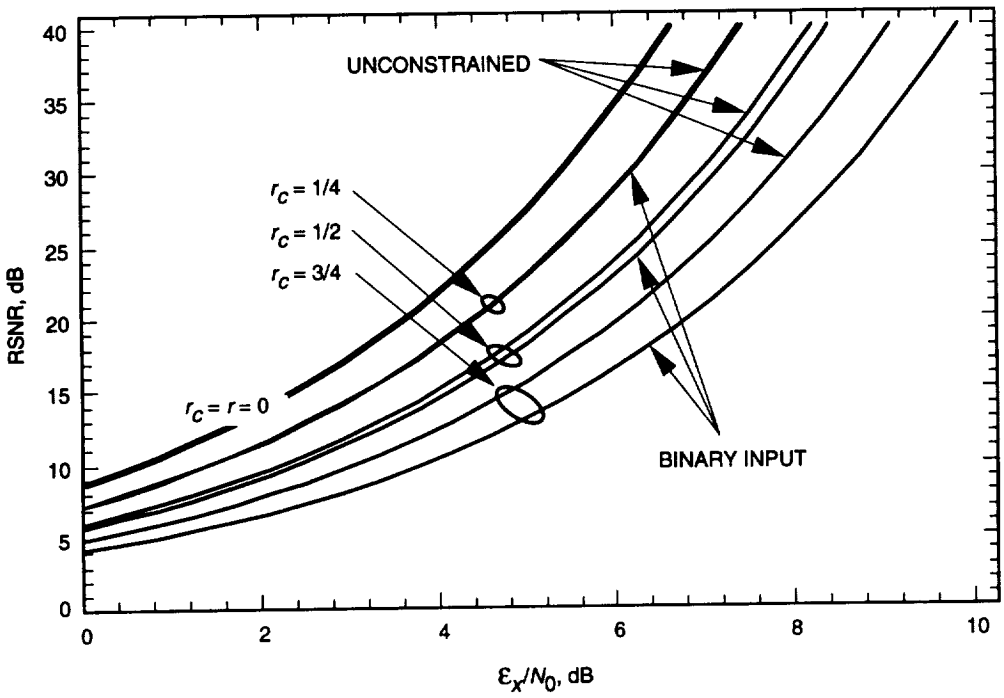

Fig. 5. Bounds on performance for binary input channel and unconstrained channel with fixed r_c.

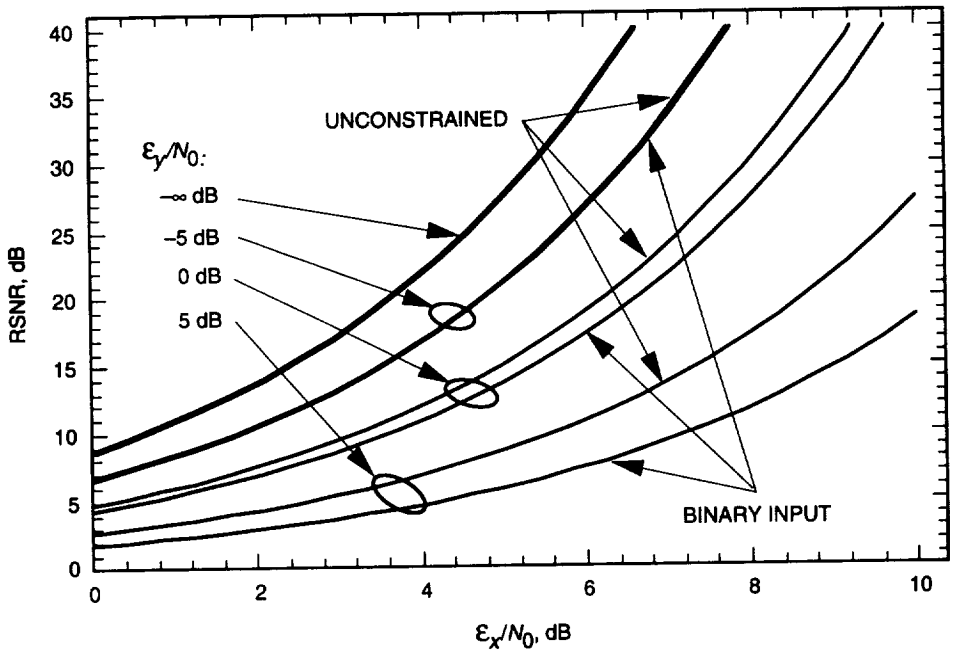

Fig. 6. Bounds on performance for binary input channel and unconstrained channel with fixed $\mathcal{E}_y/N_0$.

References

[1] C. E. Shannon, "A Mathematical Theory of Communication," *Bell System Technical Journal*, vol. 27, pp. 379–423 and 623–656, 1948.

[2] S. J. Dolinar and F. Pollara, "The Theoretical Limits of Source and Channel Coding," *The Telecommunications and Data Acquisition Progress Report 42-102, April–June 1990*, Jet Propulsion Laboratory, Pasadena, California, pp. 62–72, August 15, 1990.

[3] S. A. Butman and R. J. McEliece, "The Ultimate Limits of Binary Coding for a Wideband Gaussian Channel," *The Deep Space Network Progress Report 42-22, May–June 1974*, Jet Propulsion Laboratory, Pasadena, California, pp. 78–80, August 15, 1974.

An Efficient Implementation of Forward–Backward Least-Mean-Square Adaptive Line Enhancers

H.-G. Yeh
Spacecraft Telecommunications Equipment Section

T. M. Nguyen
Communications Systems Research Section

An efficient implementation of the forward-backward least-mean-square (FBLMS) adaptive line enhancer is presented in this article. Without changing the characteristics of the FBLMS adaptive line enhancer, the proposed implementation technique reduces multiplications by 25 percent and additions by 12.5 percent in two successive time samples in comparison with those operations of direct implementation in both prediction and weight control. The proposed FBLMS architecture and algorithm can be applied to digital receivers for enhancing signal-to-noise ratio to allow fast carrier acquisition and tracking in both stationary and nonstationary environments.

I. Introduction

Adaptive line enhancers (ALEs) are useful in many areas, including time-domain spectral estimation for fast carrier acquisition [2–4]. For example, a fast carrier acquisition technique [2],[1] as shown in Fig. 1, will be very useful for a deep-space mission, especially in a nonstationary environment or emergencies. Figure 1 is the block diagram of an ALE in a digital receiver used for both acquisition and tracking. First, the receiver is in the acquisition mode. Second, when the uplink carrier is acquired as indicated by the lock detector, the switch is shifted to the tracking position and the tracking process takes over immediately. With this acquisition scheme, the uplink carrier can be acquired by a transponder in seconds (as opposed to minutes for the Cassini transponder). Although devised to support a space mission, the architecture of the forward–backward least-mean-square (FBLMS) ALE and the associated algorithm proposed in this article are also applicable to other systems, including fixed-ground and mobile communication systems. Note that this proposed ALE scheme in the receiver needs a residual carrier, and does not work directly in suppressed-carrier cases.

A conventional ALE system using a least-mean-square (LMS) algorithm is depicted in Fig. 2, where z^{-1} represents a delay. The analysis of the ALE for enhancing the signal-to-noise ratio (SNR) to allow fast acquisition is given in [2]. The block diagram of a FBLMS adaptive line enhancer is shown in Fig. 3. The performance analysis of the FBLMS adaptive line enhancer is provided in [1]. The FBLMS adaptive line enhancer algorithm enjoys approximately half the misadjustment of that of the LMS algorithm [1].

[1] T. M. Nguyen, H. G. Yeh, and L. V. Lam, "A New Carrier Frequency Acquisition Technique for Future Digital Transponders," to be published in a future issue of *The Telecommunications and Data Acquisition Progress Report.*

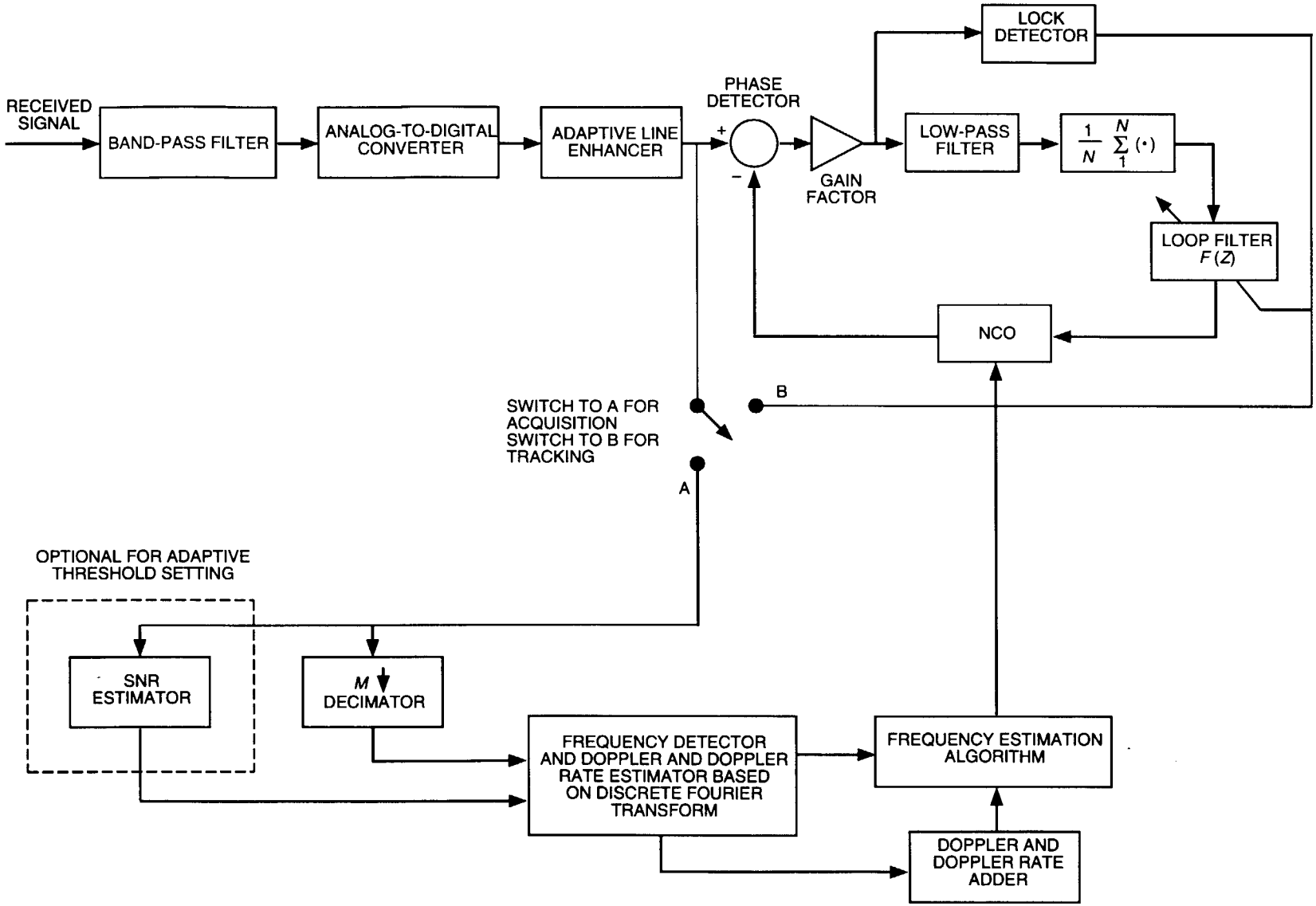

Fig. 1. The ALE in the digital receiver for both acqusition and tracking.

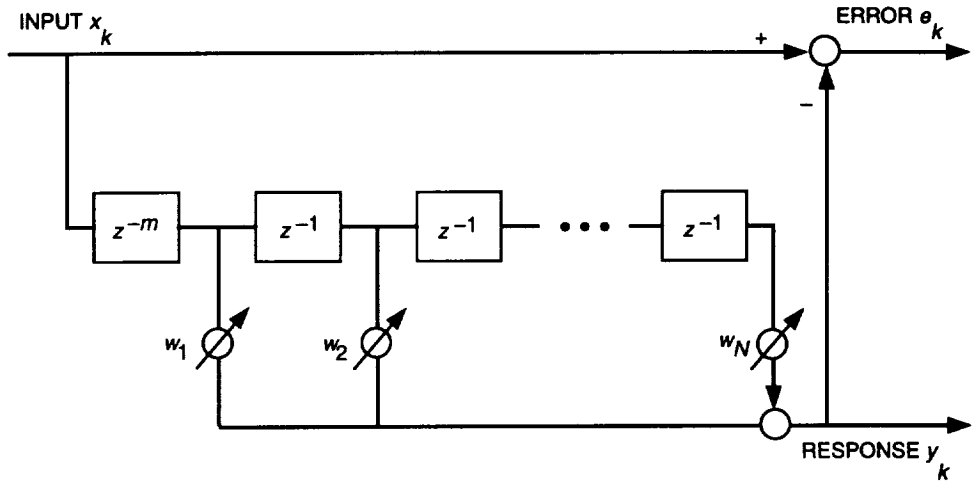

Fig. 2. The architecture of the conventional ALE.

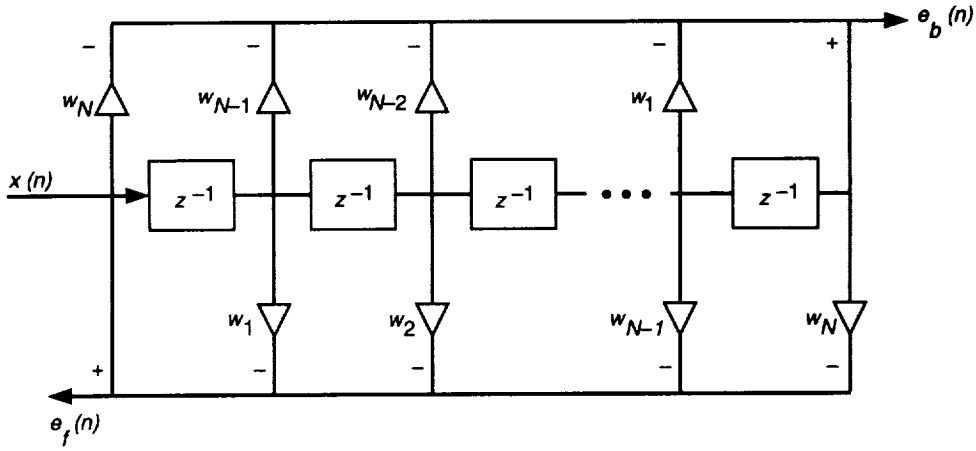

Fig. 3. The structure of the FBLMS adaptive line enhancer.

However, it requires about twice the number of multiplications and additions of the LMS algorithm. In this article, an efficient implementation of the fast FBLMS algorithm is presented. This fast algorithm provides the same speed of convergence as that of the LMS algorithm and provides the same misadjustment as that of the FBLMS adaptive line enhancer, but requires fewer multiplications and additions. The computational reduction is achieved by grouping two successive predictor computations together and computing weight adaption at every other sampling time [5]. By using a radix-2 structure to manipulate time samples, redundant computations embedded in two successive time samples can be removed via a new structure of the fast FBLMS algorithm.

This article is organized as follows. The FBLMS algorithm is reviewed in Section II. The fast FBLMS algorithm is derived and proposed in Section III. The fast FBLMS algorithm implementation is given in Section IV and simulation results are presented in Section V. Finally, the conclusion is given in Section VI.

II. Forward–Backward LMS Adaptive Line Enhancer Algorithm

The structure of the forward–backward LMS adaptive line enhancer [1] is shown in Fig. 3. The forward and backward prediction errors are then defined, respectively, as follows: